Anderson localization and quantum Hall effect: Numerical observation of two-parameter scaling

Miklós Antal Werner,[1] Arne Brataas,[2] Felix von Oppen,[3] and Gergely Zaránd[1]

[1]*MTA-BME Exotic Quantum Phases "Momentum" Research Group Department of Theoretical Physics, Budapest University of Technology and Economics, 1111 Budapest, Budafoki út 8, Hungary*

[2]*Department of Physics, Norwegian University of Science and Technology, NO-7491 Trondheim, Norway*

[3]*Dahlem Center for Complex Quantum Systems and Fachbereich Physik, Freie Universität Berlin, 14195 Berlin, Germany*

(Received 10 November 2014; revised manuscript received 17 February 2015; published 12 March 2015)

A two-dimensional disordered system of noninteracting fermions in a homogeneous magnetic field is investigated numerically. By using a modified Landau gauge, we explore the renormalization group flow of the longitudinal and Hall conductances and find that the flow is consistent with the predictions of Pruisken and Khmelnitskii. The extracted critical exponents agree with the results obtained by using transfer matrix methods. The necessity of a second scaling parameter is also demonstrated in the level curvature distribution. Near the critical point the distribution slightly differs from the prediction of random matrix theory, in agreement with previous works. Close to the quantum Hall fixed points the distribution is lognormal since here states are strongly localized.

DOI: 10.1103/PhysRevB.91.125418 PACS number(s): 72.15.Rn, 73.20.Fz, 73.43.−f, 73.50.−h

I. INTRODUCTION AND BASIC CONCEPTS

Topological phases of quantum systems have been at the focus of intense studies in recent years [1]. Many topological insulators are exotic band insulators where the energy bands are characterized by nontrivial topological quantum numbers. These topological quantum numbers reflect the nontrivial topological ground state structure, arising from the symmetries and the dimensionality of the system [2]. In a finite sample, the nontrivial topological structure of the ground state gives rise to topologically protected gapless edge states in the otherwise gapped system. These edge states are protected by topology and are robust against perturbations and disorder which do not break the underlying symmetries of the system.

One of the simplest examples of an insulating state with a nontrivial topological structure is provided by the integer quantum Hall (QH) effect [3]. In a two-dimensional electron gas, a homogeneous magnetic field splits the energy spectrum into Landau levels. For weak to intermediate disorder, Landau levels are broadened into Landau bands by disorder, and states within a Landau band are localized, except for a critical energy at the center of each band, where extended states persist [4,5]. Each Landau band is characterized by a nontrivial topological invariant, the Chern number [12]. It can be shown that the Chern number of a band—apart from a universal prefactor e^2/h—equals the contribution of the band to the Hall conductance. As a result, if the Fermi energy lies between two Landau bands, then the Hall conductance is the sum of the Chern numbers associated with the filled Landau bands. The topological character of this insulating phase is also manifested through the emergence of chiral edge states [13–16]: In fact, the total Chern number equals the number of chiral states.

As mentioned above, in each Landau band there is a critical energy ($E_{c,i}$ in the ith band) where extended states persist in the thermodynamic limit. Topologically distinct QH phases are separated by these critical states [17,18], and near them a critical behavior is observed, with the localization length (the size of the localized wave functions) diverging as

$$\xi \sim |E - E_{c,i}|^{-\nu}. \tag{1}$$

Experimentally, a quantized Hall conductance is observed if the system size (or the inelastic scattering length, $L_{\rm in}$) is much larger than the localization length at the Fermi energy, $\xi(E_F)$ [19].

The characterization of the topological quantum phase transition at these critical energies was a challenging task. Based on nonlinear σ-model calculations, Pruisken and Khmelnitskii proposed a two-parameter scaling theory, formulated in terms of the diagonal and off-diagonal elements of the dimensionless conductance tensor $g \equiv g_{xx}$ and $g_H \equiv g_{xy}$, respectively [20,21]. According to this theory, by increasing the system size L (or lowering the temperature), the conductances follow the trajectories of a two-dimensional flow diagram (see Fig. 1):

$$\frac{d\,\ln g}{d\,\ln L} = \beta(g,g_H); \quad \frac{d\,\ln g_H}{d\,\ln L} = \beta_H(g,g_H), \tag{2}$$

determined by the universal beta functions $\beta(g,g_H)$ and $\beta_H(g,g_H)$. In this flow, attractive QH fixed points appear at integer dimensionless Hall conductances and vanishing diagonal conductance. Each of these fixed points corresponds to a QH phase and is associated with a plateau in the Hall conductance. Between these attractive fixed points, other, hyperbolic fixed points emerge: these correspond to the critical state and describe transition between the QH plateaus.

There are experimental confirmations of some predictions of the universal scaling theory. However, there is only a very recent attempt of a direct numerical verification of the two-parameter renormalization group flow for ordinary QH systems. Reference [22] has investigated the temperature-driven renormalization group (RG) flow using the noncommutative Kubo formula [23]. We follow a different route and demonstrate the two-parameter scaling theory by performing finite size scaling at $T = 0$ on a lattice. These calculations are made possible by a novel lattice gauge introduced here. From the flow, we estimate the relevant and irrelevant critical exponents at the critical point, and also show the necessity of two scaling variables by investigating the distribution of level curvatures.

To perform finite size scaling, we investigate a system of noninteracting, spinless, charged fermions on a square lattice,

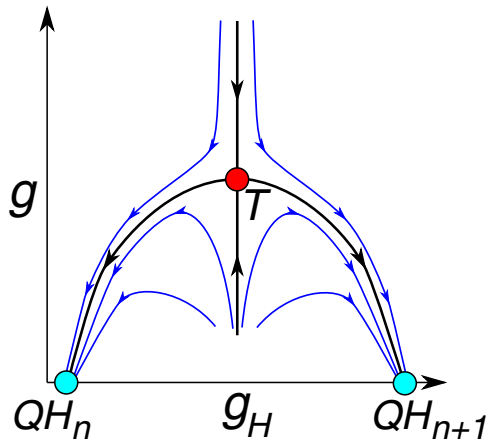

FIG. 1. (Color online) Sketch of the proposed two-parameter renormalization flow, in terms of the diagonal and Hall conductances g and g_H, respectively. The attractive QH fixed points at integer dimensionless Hall conductances and vanishing diagonal conductance are denoted by cyan circles (QH_n and QH_{n+1}). The transition fixed point (T) at a finite Hall and diagonal conductance is denoted by the red circle.

as described by the Hamiltonian

$$H = \sum_i \varepsilon_i c_i^\dagger c_i - \sum_{\langle i,j\rangle} t_{ij} c_i^\dagger c_j + \text{H.c.} \tag{3}$$

Here $c_i^\dagger$ and c_i denote fermionic operators that create or annihilate a fermion on the lattice site i, respectively. The site energies $\varepsilon_i \in [-W/2, W/2]$ are uniformly and independently distributed and the external magnetic field is introduced by using the usual Peierls substitution [29]

$$t_{ij} = e^{i2\pi A_{ij}}, \tag{4}$$

with the lattice vector potential defined as

$$A_{ij} = \frac{e}{h}\int_i^j \mathbf{A}\cdot d\mathbf{l}. \tag{5}$$

In this work, we construct a lattice gauge, which—in contrast to the Landau gauge—allows us to perform computations for small magnetic fields corresponding to a *single* flux quantum through the system. We then perform exact diagonalization at various system sizes, L, while applying twisted boundary conditions with phases ϕ_x and ϕ_y in the x and y directions, respectively. By studying the sensitivity of the energy levels $E_\alpha = E_\alpha(\underline{\phi})$ and eigenstates $|\alpha\rangle = |\alpha(\underline{\phi})\rangle$ to the phase $\underline{\phi} = (\phi_x,\phi_y)$, we are able to determine $g(L)$ and $g_H(L)$, and reconstruct the renormalization group flow, Eq. (2). We indeed find that, as predicted by Pruisken and Khmelnitskii, the flow exhibits stable QH fixed points with quantized values of g_H and $g = 0$. Neighboring QH fixed points are separated by a critical point of a finite Hall and diagonal conductance. The critical exponents extracted from the flow are in agreement with previous transfer matrix results [30].

A. Thouless formula and Hall conductance

The Kubo-Greenwood conductance formula [31] cannot be straightforwardly applied to a finite size system to extract its $T = 0$ temperature conductance in the thermodynamic limit. Fortunately, however, the Hall and the diagonal conductances can both be related to the sensitivity of the states to the boundary conditions. The single-particle eigenstates of Eq. (3) can be expanded as

$$|\alpha\rangle = \sum_i \alpha(i) c_i^\dagger |0\rangle\,. \tag{6}$$

Labeling for the moment each site i by its coordinates $i \to x,y$, a twisted boundary condition is defined by wrapping the system on a torus with the periodicity condition

$$\alpha(x + nL, y + mL) = e^{i(n\phi_x + m\phi_y)}\alpha(x,y). \tag{7}$$

The phases $(\phi_x,\phi_y) = \underline{\phi}$ can be interpreted as magnetic fluxes pierced through the torus (and in its interior), while the external magnetic field pierces through the surface of the torus (see Fig. 2). Solving the eigenvalue equation $H|\alpha\rangle = E_\alpha|\alpha\rangle$, one obtains the phase dependent eigenstates and eigenvalues $|\alpha(\underline{\phi})\rangle$ and $E_\alpha(\underline{\phi})$.

In a seminal work, Thouless and Edwards conjectured a relation between the diagonal conductance and the mean absolute curvature of eigenenergies at the Fermi energy [24,32],

$$g \approx g_T = \overline{|c_T(\alpha)|}_{E_\alpha = E_F}, \quad c_T(\alpha) = \frac{\pi}{\Delta(E_\alpha)}\frac{\partial^2 E_\alpha}{\partial \phi_x^2}, \tag{8}$$

with $\Delta(E_F)$ denoting the mean level spacing at the Fermi energy, and the overline indicating disorder averaging. Although this formula cannot be derived rigorously, it has been verified numerically for a wide range of disorder [33].

The Hall conductance can be directly related to the phase dependence of the eigenstates [34]. In a finite system, the

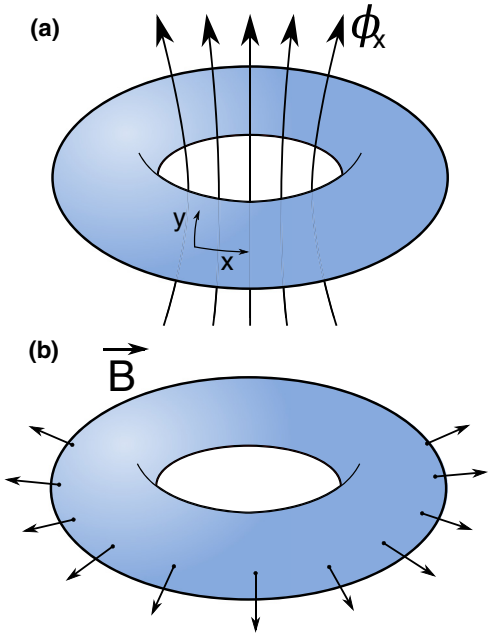

FIG. 2. (Color online) (a) The phase ϕ_x can be interpreted as a magnetic flux pierced through the torus. (b) The external magnetic field pierces through the surface of the torus.

average Hall conductance at $T = 0$ is

$$g_H = \overline{\sum_{E_\alpha < E_F} c_H(\alpha)}. \tag{9}$$

Here $c_H(\alpha)$ denotes the Hall conductance of level $|\alpha\rangle$, and is given by

$$c_H(\alpha) = 2\pi i \left(\left\langle \frac{\partial \alpha}{\partial \phi_y} \middle| \frac{\partial \alpha}{\partial \phi_x} \right\rangle - \left\langle \frac{\partial \alpha}{\partial \phi_x} \middle| \frac{\partial \alpha}{\partial \phi_y} \right\rangle \right), \tag{10}$$

the Berry curvature associated with $|\alpha(\phi_x, \phi_y)\rangle$. In the following, we shall use Eqs. (8) and (9) to determine the dimensionless conductances and establish the flow.

B. Lattice gauge for small magnetic fields

In a finite size system with periodic or twisted boundary condition, a homogeneous magnetic field cannot be arbitrary; the hopping matrix elements must respect the periodicity of the system, i.e., the hoppings at sites $(x + L, y)$ and $(x, y + L)$ must be equal with the one at (x, y). The complex phases of the hopping matrix elements are related to the magnetic vector potential through the Peierls substitution, Eq. (4).

The periodicity of the system requires the complex phase of the hopping to be changed by $2\pi n$ as the x or y coordinates are shifted by L, and imposes restrictions on the total field pierced through the system.

The magnetic flux through a unit cell can be determined by summing the hopping phases around the cell, while the magnetic field in a cell can be defined as the flux divided by the area of the cell. Setting the lattice size to $a = 1$, the magnetic field reads

$$B_{(x+1/2,\, y+1/2)} = \frac{h}{e}[A_{(x,y)(x+1,y)} + A_{(x+1,y)(x+1,y+1)} + A_{(x+1,y+1)(x,y+1)} + A_{(x,y+1)(x,y)}]. \tag{11}$$

Periodic boundary conditions imply that the total magnetic flux through the whole system is a multiple of the flux quantum $\Phi_0 = h/e$. Therefore, the minimal nonzero magnetic flux through the system [the surface of the torus in Fig. 2(b)] is Φ_0. Most numerical calculations use the Landau gauge with $A^{\text{Landau}}_{(x,y),(x,y+1)} = \frac{x}{L}\, m$ with m an integer and $A^{\text{Landau}}_{(x,y),(x+1,y)} = 0$, which results in a total flux

$$\Phi_{\text{Landau}} = mL\Phi_0 \tag{12}$$

through the system. The minimal nonzero flux in the Landau gauge is thus L times larger than the flux quantum Φ_0, and consequently, the possible values of magnetic field, $B_{\text{Landau}} = \frac{\Phi_{\text{Landau}}}{L^2} = \frac{m}{L}\,\Phi_0$, are restricted and rather large.

Clearly, to perform efficient finite size scaling at a fixed magnetic field, one needs to construct a lattice gauge, which is able to produce magnetic fields below the Landau gauge limit, $B^{\text{min}}_{\text{Landau}} = \frac{1}{L}\Phi_0$. Here we propose to use a lattice gauge, as illustrated in Fig. 3, that realizes the minimal flux and the corresponding minimal magnetic field. Along the y bonds, we use a Landau gauge

$$A_{(x,y)(x,y+1)} = m\frac{x}{L^2}, \quad x \in 1 \ldots L. \tag{13}$$

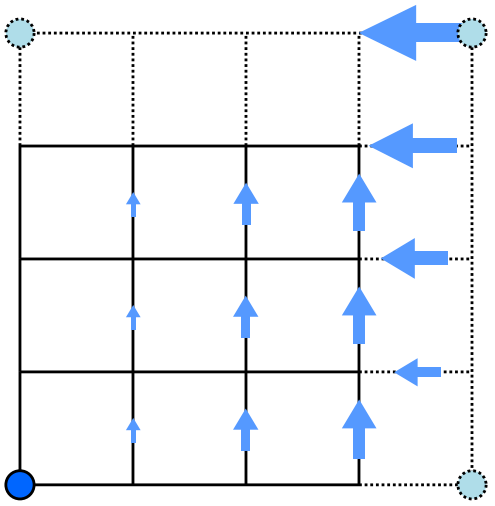

FIG. 3. (Color online) Sketch of bond vector potentials on a 4×4 lattice with periodic boundary condition: The circles denote equivalent sites.

This is by a factor $1/L$ smaller than the usual Landau gauge and, consequently, amounts in an additional jump in the phase of the hopping between lattice sites $x = L$ and $x = 1$, $\Delta\varphi = -2\pi\, m\frac{1}{L}$. Such a jump would introduce a strong magnetic field at the boundaries, if it is not compensated. Therefore at the boundary between $x = L$ and $x = 1$, we apply a lattice vector potential in the x direction [35]

$$A_{(x=L,y)(x=1,y)} = -m\frac{y}{L}. \tag{14}$$

One can verify that the magnetic field in each cell is Φ_0/L^2, therefore the total magnetic flux is just the minimal nonzero flux Φ_0. Using this gauge, we can thus reach magnetic field values of $B = \frac{m}{L^2}\,\Phi_0$, allowing us to change the system size in relatively small steps when the magnetic field is fixed.

II. RESULTS

A. RG flow and critical behavior

Let us start by analyzing the critical behavior of the dimensionless conductances. The Thouless and Hall conductances were calculated for system sizes between $L = 9$ and $L = 33$, magnetic fields $B = 1/9$, $1/4$, and $1/16$ (in units of Φ_0/a^2), and disorder strengths $1 \leqslant W \leqslant 3.5$. A total number of $\sim 5 \times 10^8$ eigenstates were computed for each system size, magnetic field, and disorder. The behavior of the ensemble averaged conductances as a function of the Fermi energy is shown in Fig. 4. The Hall step becomes sharper with increasing system size and the peak in the Thouless conductance gets sharper as well.

Based upon the two-parameter scaling theory, near the transition, the dimensionless Hall conductance is expected to scale with the system size as

$$g_H(L') - g_H^* \cong \left(\frac{L'}{L}\right)^y (g_H(L) - g_H^*), \tag{15}$$

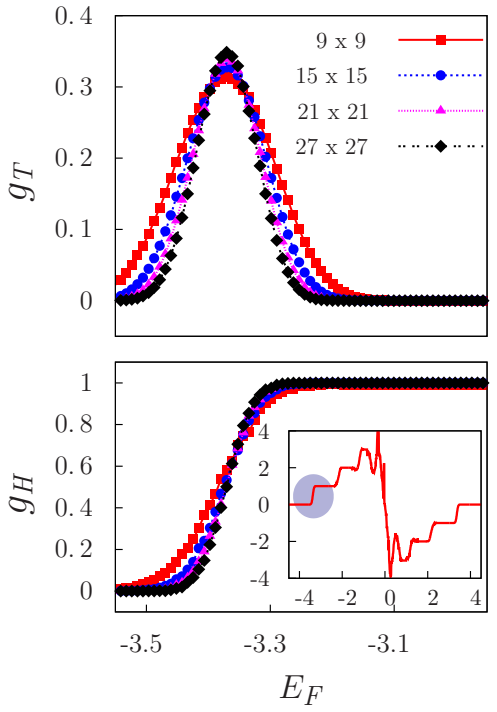

FIG. 4. (Color online) Thouless conductance (upper panel) and Hall conductance (lower panel) as a function of Fermi energy around the first Landau band for $B = \Phi_0/9$ and $W = 1$. System sizes are $L = 9$, 12, 18, and 27. *Inset:* Hall conductance g_H as a function of the Fermi energy E_F in the whole band. The shaded region highlights the first QH step, shown in the main panel. In the lower half of the band electronlike behavior is observed, while in the upper half holelike behavior is observed.

where y is the scaling dimension of the Hall conductance, and g_H^* denotes the critical Hall conductance. In contrast, the Thouless conductance is predicted to be an irrelevant scaling variable on the critical surface, where

$$g_T(L') - g_T^* \cong \left(\frac{L'}{L}\right)^{-|y_2|} [g_T(L) - g_T^*], \qquad (16)$$

with y_2 the scaling dimension of the leading irrelevant operator. We estimated the critical values of the Hall and Thouless conductances and the exponents y and y_2 by performing a finite size scaling analysis, yielding

$$g_H^* = 0.612 \pm 0.023, \quad y = 0.351 \pm 0.082, \qquad (17)$$

and

$$g_T^* = 0.386 \pm 0.011, \quad |y_2| = 0.43 \pm 0.14. \qquad (18)$$

The critical exponents y and y_2 agree within our numerical accuracy with the values $y = 1/\nu \approx 0.385$ and $|y_2| \approx 0.4$, extracted through transfer matrix methods [30,36–38].

The system size driven (g_T, g_H) flow is displayed in Fig. 5. Of course, due to numerical errors, the flow is not perfect and certain lines (arrows) seem to cross, but the qualitative agreement with the Pruisken-Khmelnitskii scaling is apparent. As mentioned before, the modified Landau gauge enables us to increase the system size in smaller steps, and to get a better resolution of the β functions. Nevertheless,

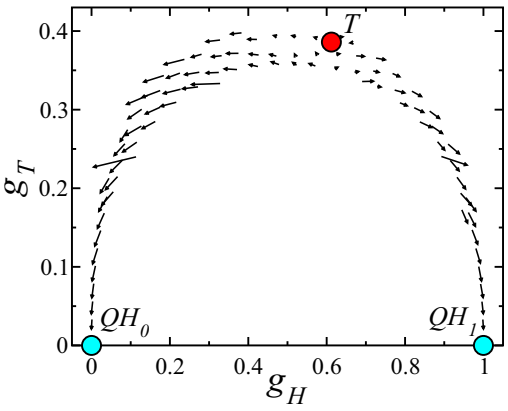

FIG. 5. (Color online) Two-parameter renormalization flow extracted from finite size scaling for $B = \Phi_0/4$, $W \in 2 \ldots 3.3$ and $L \in 12 \ldots 24$. The arrows show the direction of increasing system size. The extrapolated position of the critical point is denoted by a red circle (T); the zeroth and first QH fixed points are denoted by a cyan circle (QH_0 and QH_1).

it remains challenging to collect data from the exterior or deep interior of the critical dome (flipped "U" shape), because the trajectories remain always close to it. Interestingly, the flow is slightly asymmetrical, and the critical point is closer to the $n = 1$ QH state than the trivial $n = 0$ state. We do not have a firm explanation for this asymmetry. The lack of electron-hole symmetry could provide a natural explanation of such asymmetry. However, the fact that the flows extracted for various fillings overlap within our numerical accuracy, may rule out this possibility. The observed asymmetry may also be a peculiarity of lattice calculations or nonuniversal finite size corrections, associated with the presence of other irrelevant operators, resulting in deviations from the universal scaling curves for smaller system sizes.

The system sizes we used here are somewhat smaller than those in Ref. [22]. This is because for the Hall conductance we need to compute the full spectrum of the system, and the long tailed distributions of the Thouless and Hall conductances require averaging over a large ensemble of disorder realizations ($n \sim 10^6$ samples), limiting the accessible system sizes. In contrast, in the approach of Ref. [22] a relaxation time is implicitly included. This probably implies an automatic internal averaging/smoothening, and therefore a smaller number of disorder realizations ($n \sim 100$) and, consequently, larger system sizes can be employed. Despite this difference, however, the relaxation time driven flow of Ref. [22] and the system size driven flow presented here appear to be of similar numerical quality.

B. Curvature distributions

The presence of two characteristic scaling variables is also clear from a careful analysis of the distribution of level resolved Hall conductances and Thouless curvatures. Single-parameter scaling [39] would imply that these distributions should be characterized by a single dimensionless parameter, which we can choose to be the Thouless conductance, $g_T = g_T(W, E, L, B, \ldots)$. To test the single-parameter scaling hypothesis, we selected regions in the energy spectra

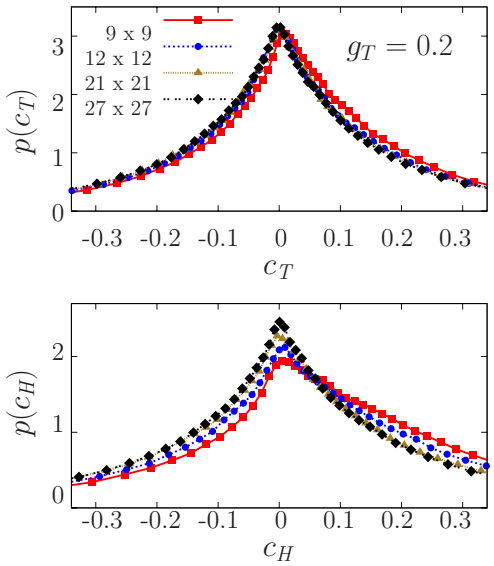

FIG. 6. (Color online) Distribution of the Thouless curvature (upper panel) and the level resolved Hall conductance (lower panel). We used $B = 1/9$ and $W = 1$, and varied the system size (see legend). For each system size we selected energy regions corresponding to a fixed $g_T = 0.2$, and determined the distributions for a large number of disorder realizations. Distributions for a fixed g_T depend explicitly on the system size, L, but converge to a limiting distribution for large L (see data for $L = 21$ and 27).

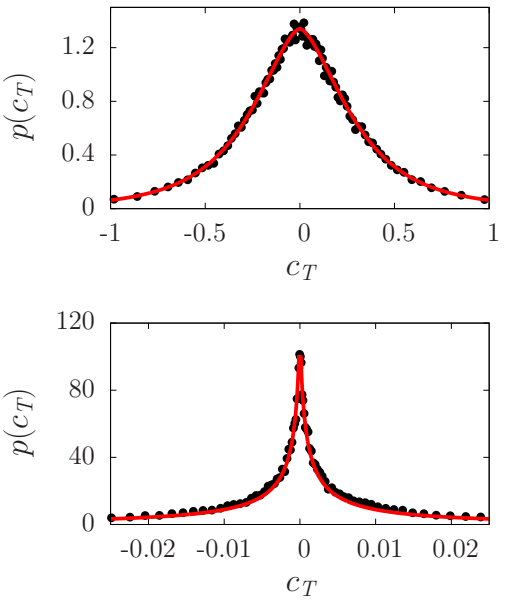

FIG. 7. (Color online) Curvature distributions in the vicinity of the transition fixed point (upper panel, $g_T \approx 0.35$, $g_H \approx 0.55$), and close to the quantum Hall fixed points (lower panel, $g_T \approx 0.003$, $g_H \approx 0.001$). Continuous lines denote modified Cauchy (top) and lognormal (bottom) fits.

with a fixed Thouless conductance, g_T (i.e., fixed average absolute curvature $\overline{|c_T|}$), and determined the distributions $p(c_T|g_T,L,W,B)$ and $p(c_H|g_T,L,W,B)$ [40]. We found that the single-parameter scaling hypothesis is clearly violated for small system sizes; both $p(c_T)$ and $p(c_H)$ depend explicitly on the system size, L. The explicit L dependence is more pronounced in the distribution of the level resolved Hall conductance, but can also be seen in the distribution of the level curvatures. Increasing L, however, the distributions converge to a limiting distribution (see data for $L = 21$ and 27 in Fig. 6). This behavior can be understood in terms of the two-parameter scaling theory. According to the latter, the distributions $p(c_T)$ and $p(c_H)$ depend on two dimensionless parameters, g_T and g_H: $p(c_T) = p(c_T|g_T,g_H)$ and $p(c_H) = p(c_H|g_T,g_H)$. For a given value of g_T, increasing L moves the corresponding (g_T,g_H) point towards the flipped "U" envelope in the (g_T,g_H) plane. That means that for systems with large L, g_H becomes effectively a function of g_T, $g_H \to g_H(g_T)$, and therefore $p(c_T)$ depends solely on g_T.

The distributions $p(c_T)$ and $p(c_H)$ vary considerably within the (g_T,g_H) plane (see Fig. 7). Near the transition point, the distribution of the dimensionless Thouless curvatures can be well fitted by a modified Cauchy distribution,

$$p(c_T) \propto \frac{1}{\left(c_T^{\kappa} + a\right)^{(2+\beta)/\kappa}}, \tag{19}$$

with the constant $\beta = 2$ characterizing the unitary ensemble, and κ a symmetry class dependent anomalous dimension. Such a distribution has been conjectured for the critical curvature distribution in orthogonal and unitary ensembles, and verified numerically for the orthogonal case [41,42]. By fitting the numerically obtained distributions, we extract an exponent

$$\kappa = 1.603 \pm 0.026. \tag{20}$$

This value is close to the exponent $\kappa = 2$, predicted for disordered metallic systems in the unitary ensemble by random matrix theory [43,44]. In fact, although a modified Cauchy distribution is needed to reach a high quality fit of the small curvature part of the distribution, the random matrix expression ($\kappa = 2$) also provides an acceptable fit of the data.

Close to the attractive quantum Hall fixed points, on the other hand, the dimensionless curvature is lognormally distributed with a good accuracy, a behavior characteristic of strongly localized states [45].

III. CONCLUSION

In this work, we investigated disordered Quantum Hall systems by performing numerical computations within a torus geometry. We constructed a magnetic gauge, which enabled us to reach the smallest magnetic field allowed by the periodic boundary condition, $B = \frac{1}{L^2}\frac{h}{e}$. With this gauge, we were able to increase the system size in smaller steps, and could perform efficient finite size scaling.

We determined the boundary condition (phase) dependence of the eigenstates and eigenenergies, and computed from these the diagonal and Hall conductances. We established the system size driven renormalization group flow of the dimensionless Hall conductance and the Thouless conductance, and found it to be consistent with the theoretical predictions of Pruisken and Khmelnitskii. We identified the quantum Hall fixed points, responsible for the quantized values of the Hall conductance, and the critical fixed point characterizing the transition between neighboring quantum Hall phases. In the

vicinity of this critical point, the Hall conductance is found to be a relevant scaling variable, while the diagonal conductance becomes irrelevant. We estimated the critical exponents of the transition fixed point, and found them to agree with the values calculated using transfer matrix methods.

Our results agree with those obtained via another path of Ref. [22], where the temperature dependence of the conductances, computed by means of the noncommutative Kubo formula, has been used to generate the RG flow. While the overall quality of the RG flow we obtain is similar to that of Ref. [22], in our case, the RG flow exhibits a slight asymmetry, which seems to be almost absent in Ref. [22]. The observed electron-hole asymmetry of the flow is probably due to the relatively small system sizes we used, and to the presence of irrelevant operators.

We also investigated the distributions of level curvatures, and observed a clear violation of the one-parameter scaling, demonstrating the necessity of a second parameter. For large system sizes, however, the system flows towards a critical line, and the single-parameter scaling is found to be restored, in agreement with the Pruisken-Khmelnitskii scaling theory. Near the critical point, the distribution of the Thouless curvature is found to agree with the predictions of random matrix theory (Gaussian unitary ensemble). Close to the quantum Hall points the curvature distribution is lognormal.

ACKNOWLEDGMENTS

This research has been supported by the Hungarian Scientific Research Fund OTKA under Grants No. K105149 and No. CNK80991. We also acknowledge the support of the Helmholtz Virtual Institute "New states of matter and their excitations" as well as the DFG Schwerpunkt 1666 Topological Insulators, and a DFG Mercator Guest Professorship.

[1] M. Z. Hasan and C. L. Kane, Rev. Mod. Phys. **82**, 3045 (2010).
[2] A. Kitaev, in *Advances in Theoretical Physics: Landau Memorial Conference*, edited by V. Lebedev and M. Feigel'man, AIP Conf. Proc. No. 1134 (AIP, NY, 2009), p. 22.
[3] K. v. Klitzing, G. Dorda, and M. Pepper, Phys. Rev. Lett. **45**, 494 (1980).
[4] H. Aoki and T. Ando, Solid State Commun. **38**, 1079 (1981).
[5] This picture needs to be modified for large disorder or very small magnetic fields. If the amount of disorder is higher or the magnetic field is weaker than a critical value, then all states become localized and the nontrivial topological structure is destroyed. For a disordered electron gas in a weak magnetic field Khmelnitskii and Laughlin argued that the critical states should simply drift above the Fermi energy at very small fields (see Refs. [6,7]). The fate of the extended states on a lattice remained, however, unclear: In an early work, Yang and Bhatt argued that extended states merge for large disorder (see Ref. [8]). While some works appear to confirm "levitation" towards the center of the band (see Refs. [9,10]), other studies seem to indicate a drift towards the band edge upon increasing disorder in a weak field (see Ref. [11]).
[6] R. B. Laughlin, Phys. Rev. Lett. **52**, 2304 (1984).
[7] D. E. Khmelnitskii, Phys. Lett. A **106**, 182 (1984).
[8] K. Yang and R. N. Bhatt, Phys. Rev. B **59**, 8144 (1999).
[9] Th. Koschny and L. Schweitzer, Phys. Rev. B **70**, 165301 (2004).
[10] A. L. C. Pereira and P. A. Schulz, Phys. Rev. B **66**, 155323 (2002).
[11] C. Wang, Y. Avishai, Y. Meir, and X. R. Wang, Phys. Rev. B **89**, 045314 (2014).
[12] D. J. Thouless, M. Kohmoto, M. P. Nightingale, and M. den Nijs, Phys. Rev. Lett. **49**, 405 (1982).
[13] N. Goldman, J. Dalibard, A. Dauphin, F. Gerbier, M. Lewenstein, P. Zoller, and I. B. Spielman, Proc. Natl. Acad. Sci. U. S. A. **110**, 6736 (2013).
[14] N. Aoki, C. R. da Cunha, R. Akis, D. K. Ferry, and Y. Ochiai, Phys. Rev. B **72**, 155327 (2005).
[15] N. Ofek, A. Bid, M. Heiblum, A. Stern, V. Umansky, and D. Mahalu, Proc. Natl. Acad. Sci. U. S. A. **107**, 5276 (2010).
[16] K. C. Nowack, E. M. Spanton, M. Baenninger, M. König, J. R. Kirtley, B. Kalisky, C. Ames, P. Leubner, C. Brüne, H. Buhmann, L. W. Molenkamp, D. Goldhaber-Gordon, and K. A. Moler, Nat. Mater. **12**, 787 (2013).
[17] B. I. Halperin, Phys. Rev. B **25**, 2185 (1982).
[18] B. Huckestein, Rev. Mod. Phys. **67**, 357 (1995).
[19] The Hall conductance can have nonquantized values, however, if the localization length at the Fermi energy is larger than other length scales.
[20] A. M. M. Pruisken, Phys. Rev. Lett. **61**, 1297 (1988).
[21] D. E. Khmel'nitskii, Pis'ma Zh. Eksp. Teor. Fiz. **38**, 454 (1983) [JETP Lett. **38**, 552 (1983)].
[22] J. Song and E. Prodan, Eur. Phys. Lett. **105**, 37001 (2014).
[23] The two-parameter scaling has been studied numerically, however, for Dirac fermions and topological insulators in Refs. [24–28].
[24] K. Nomura, S. Ryu, M. Koshino, C. Mudry, and A. Furusaki, Phys. Rev. Lett. **100**, 246806 (2008).
[25] K. Nomura and N. Nagaosa, Phys. Rev. Lett. **106**, 166802 (2011).
[26] T. Morimoto and H. Aoki, Phys. Rev. B **85**, 165445 (2012).
[27] R. S. K. Mong, J. H. Bardarson, and J. E. Moore, Phys. Rev. Lett. **108**, 076804 (2012).
[28] Y. Xue and E. Prodan, Phys. Rev. B **87**, 115141 (2013).
[29] R. Peierls, Z. Phys. **80**, 763 (1933).
[30] K. Slevin and T. Ohtsuki, Phys. Rev. B **80**, 041304 (2009).
[31] R. Kubo, J. Phys. Soc. Jpn. **12**, 570 (1957).
[32] J. T. Edwards and D. J. Thouless, J. Phys. C. **5**, 807 (1972).
[33] D. Braun, E. Hofstetter, G. Montambaux, and A. MacKinnon, Phys. Rev. B **55**, 7557 (1997).
[34] Q. Niu, D. J. Thouless, and Y.-S. Wu, Phys. Rev. B **31**, 3372 (1985).
[35] Inside the system $A_{(x,y)(x+1,y)} = 0$ for $x = 1 \ldots L - 1$.
[36] B. Huckestein, Phys. Rev. Lett. **72**, 1080 (1994).
[37] H. Obuse, I. A. Gruzberg, and F. Evers, Phys. Rev. Lett. **109**, 206804 (2012).
[38] I. C. Fulga, F. Hassler, A. R. Akhmerov, and C. W. J. Beenakker, Phys. Rev. B **84**, 245447 (2011).

[39] E. Abrahams, P. W. Anderson, D. C. Licciardello, and T. V. Ramakrishnan, Phys. Rev. Lett. **42**, 673 (1979).
[40] The Thouless curvature fluctuates from level to level and also depends on the specific disorder configuration.
[41] C. M. Canali, C. Basu, W. Stephan, and V. E. Kravtsov, Phys. Rev. B **54**, 1431 (1996).
[42] The verification of ansatz (19) has been problematic for the unitary ensemble [see Y. Avishai and R. Berkovits, Phys. Rev. B. **55**, 7791 (1997)].
[43] F. von Oppen, Phys. Rev. Lett. **73**, 798 (1994).
[44] F. von Oppen, Phys. Rev. E **51**, 2647 (1995).
[45] M. Titov, D. Braun, and Y. V. Fyodorov, J. Phys. A. **30**, 339 (1997).